HHS Public Access

Author manuscript

Circ Cardiovasc Imaging. Author manuscript; available in PMC 2022 June 09.

Published in final edited form as:

Circ Cardiovasc Imaging. 2021 June ; 14(6): e012549. doi:10.1161/CIRCIMAGING.121.012549.

PET Imaging of Regional vs Global Myocardial Sympathetic Activity to Improve Risk Stratification in Patients with Ischemic Cardiomyopathy

Jason G. E. Zelt, PhD[#a,b,c], **Jean Zhuo Wang, BHSc**[#a,b], **Lisa M. Mielniczuk, MSc MD**[a,b,c], **Rob S.B. Beanlands, MD**[a,b], **James A. Fallavollita, MD**[d,e], **John M. Canty Jr., MD**[d,e], **Robert A. deKemp, PhD**[a,b]

[a]Department of Medicine (Cardiology), University of Ottawa Heart Institute, Ottawa, Canada

[b]Faculty of Medicine, University of Ottawa, Ottawa, Canada

[c]Department of Cellular and Molecular Medicine, University of Ottawa, Ottawa, Canada

[d]VA Western New York Healthcare System, Buffalo, NY, USA.

[e]Division of Cardiovascular Medicine, University of Buffalo, Buffalo, NY, USA

[#] These authors contributed equally to this work.

Abstract

Background: Current risk assessment approaches fail to identify the majority of patients at risk of sudden cardiac arrest (SCA). Non-invasive imaging of the cardiac sympathetic nervous system (SNS) using SPECT and PET offers the potential for refining SCA risk assessment. While various [^{11}C]meta-hydroxyephedrine (HED) quantification parameters have been proposed, it is currently unknown whether regional denervation or global innervation yields greater SCA risk discrimination. The aim of the study was to determine whether the global innervation parameters yield any independent and additive prognostic value over the regional denervation alone.

Methods: In a *post hoc* competing risks analysis of the PAREPET trial, we compared global innervation and regional denervation parameters using the norephinephrine analog HED for SCA risk discrimination. Patients with ischemic cardiomyopathy (n=174) eligible for an implantable cardiac defibrillator (ICD) for the primary prevention of SCA were recruited into the trial. HED uptake and clearance rates were measured to assess global (LV mean) retention index (RI) and volume of distribution (DV). Regional defects were quantified as the percentage of the LV having values <75% of the maximum.

Results: During a median follow-up of 4.2 years, there were 56 cardiac related deaths, of which 26 were SCAs. For any given regional denervation volume there was substantial heterogeneity in global innervation scores. Global RI and DV did not decrease until regional defects exceeded 40%

Address for Correspondence: Dr. Robert deKemp, 40 Ruskin Street, Ottawa, Ontario, Canada, K1Y 4W7, RAdeKemp@ottawaheart.ca, Fax 613-696-7104; Phone 613-696-7347.

Disclosures: RSB is a consultant for- and has received grant funding from GE Healthcare, Lantheus Medical Imaging and Jubilant DraxImage (JDI). RAdK is a consultant for JDI and receives royalties from Rubidium PET technologies licensed to JDI and to INVIA Medical Solutions. JMC is a consultant for Lantheus Medical Imaging. The other authors, JGEZ, JZW, and JAF have no disclosures.

LV. Global scale parameters, RI and DV (AUC=0.61, p=0.034, p=0.046, respectively), yielded inferior SCA risk discrimination compared to regional heterogeneity (AUC=0.74).

Conclusion: Regional denervation volume has superior cause-specific mortality prediction for SCA versus global parameters of sympathetic innervation. These results have widespread implications for future cardiac sympathetic imaging, which will greatly simply innervation analysis.

Introduction

Sudden cardiac arrest (SCA) remains a lethal and unpredictable event, accounting for half of all heart related deaths.[1] Survivors of myocardial infarction (MI) have a four-fold elevated risk of arrhythmic death compared to persons without a history of MI.[2] Clinically, ejection fraction (EF) is the main parameter used to delineate risk and guide the need for primary prevention ICD therapy (EF≤35%).[3] Yet, the long-term appropriate discharge rate among these patients is only 11-35% over a 3-4 year period.[4-6] Furthermore, despite lower rates of SCA in patients with LVEF>35%, this population actually accounts for the majority of SCA cases.[7] Non-invasive imaging of the cardiac sympathetic nervous system (SNS) has been proposed to compliment SCA risk assessment. This may not only enable more cost-effective patient selection and improved outcomes, but also provide a way to identify the large number of patients that develop SCA with an EF >35%.

Alterations in the sympathetic nervous system have been implicated in the development of lethal ventricular arrhythmias.[8-14] These can arise from global alterations in myocardial sympathetic tone without structural alterations in sympathetic nerve density. In addition, since sympathetic nerves are exquisitely sensitive to ischemia and infarction, regional defects can develop with the zone of denervation often extending beyond the ischemic penumbra.[15]

Both positron emission tomography (PET) and single photon emission computed tomography (SPECT) tracers have been developed to characterize the cardiac sympathetic nervous system. Of them, ^{123}I-meta-iodobenzylguanidine (MIBG) for SPECT and planar imaging and [^{11}C]*meta*-hydroxyephedrine (HED) for PET have been most widely studied in large prospective trials. The ADMIRE-HF trial used planar MIBG imaging for predicting cardiac events in patients with LVEF<35%.[12] The heart-to-mediastinum (H/M) ratio was assessed, serving as a global index of SNS dysfunction. In this trial, a H/M<1.6 portents a worsening prognosis. In contrast, the PAREPET trial (Prediction of ARrhythmic Events with Positron Emission Tomography) demonstrated that regional sympathetic denervation volume, assessed using HED PET, predicts SCA independently of LVEF and infarct volume.[15] The superior spatiotemporal resolution and well validated attenuation correction for PET enables the separate quantification of global scale and regional heterogeneity.

Various methods of HED quantification for positron emissions tomography (PET) have been proposed to assess the burden of sympathetic denervation and dysfunction. While these methods may require varying degrees of quantitative sophistication and imaging time, there remains a paucity of research evaluating which method yields the most robust SCA risk discrimination. Quantification of both global (i.e. total tracer uptake and retention) and

regional (i.e. defect volume) sympathetic innervation have been reported in the literature, but lack direct comparisons with prognosis data. The PAREPET trial calculated a regional uptake defect score, expressed as percentage of the total left ventricle (LV).[15] In contrast, other studies report global parameters with HED quantification of tracer retention index (RI) and/or volume of distribution (DV). While there is some debate as to which better reflects global cardiac sympathetic innervation[16-20], initial reports suggest DV may be less flow-dependent and thus may be a more relevant parameter, particularly for patients with ischemic cardiomyopathy.[20] Conceptually, patients with a given defect size may have varying degrees of global LV uptake. Mechanistically, this may be due to differing defect severities, heterogenous uptake in remote regions or a global reduction in tracer uptake. To date, no study has determined the prognostic significance of global tracer uptake parameters, independent of defect size and whether they offer any additive value in SCA risk prediction.

The objectives of the present analysis were two-fold: 1) in a competing-risk analysis compare the robustness of regional and global [^{11}C]HED quantification parameters for predicting cause-specific mortality from SCA and 2) determine whether the global RI and DV assessments yield any independent and additive prognostic value over the regional defects alone.

Methods

The data in the present analysis will not be made available to other researches as this was not included in the original patient consent form in the PAREPET trial.

Study Population

The PAREPET trial (NCT01400334) enrolled 204 subjects with ischemic cardiomyopathy, eligible for an ICD for primary prevention of SCA. [15] The University of Buffalo Institutional Review Board approved the study protocol and all subjects signed an informed consent form. Of the 204 participants, 190 patients underwent HED PET scans. N=16 were excluded from the present study due to reasons listed in Figure 1, leaving n=174 included for analysis.

PET Imaging

PET imaging was performed as described in prior methods.[15,21] An intravenous bolus of 740 MBq (20 mCi) of HED was administered, followed by dynamic cardiac PET imaging for 60 minutes (6×30 sec, 2×60 sec, 2×150 sec, 2×300 sec, 2×600 sec, 1×1200 sec frames). The images were reconstructed with all corrections enabled using filtered back-projection and a Hann window of the Ramp filter, resulting in ~10 mm isotropic resolution. Dynamic Images were analyzed using FlowQuant® v2.4 (University of Ottawa Heart Institute, Ottawa, Canada).

HED Parameters

Retention Index—Retention index is a measure utilized to estimate the net uptake of HED at scan end-time, calculated using the following equation which relates the activity in myocardial tissue (C_m) to the unchanged tracer activity in plasma (C_p) and the function evaluation time (T_R):

$$RI_{(RC)} = \frac{C_m(T_R)}{\int_0^{T_R} C_p(t)dt} \times 100\,\% \quad (1)$$

No partial-volume recovery correction was applied (*RC=1*) as fractional blood volume is not estimated using the retention model.

Distribution Volume—The distribution volume is defined as the ratio of tracer concentration in the myocardium to arterial plasma, at equilibrium. For receptor ligands, the DV physiologically reflects tracer binding affinity (i.e. B_{max}/K_d), where B_{max} is Uptake1 density and $1/K_d$ is the affinity of HED for the Uptake1 transporter. [22] Volumes of distribution were calculated using a one-tissue compartment model as previously described. [23] This method can be expressed by the following equation, where C_m is myocardial tracer concentration, C_p is arterial plasma tracer concentration, and T_E is the time to equilibrium:

$$DV = \frac{K_1}{k_2} = \frac{C_m(T_E)}{C_p(T_E)} \quad (2)$$

Quantitative analysis requires subtraction of radiolabeled blood metabolites accumulating in the blood stream to ensure accurate computation. The arterial whole-blood time-activity curve was obtained from a 20 mm^3 region in the LV cavity. The following equation was used to correct for blood metabolites: $C_p(t) = C_{wb}(t) \times pfp(t)$, where $C_p(t)$ is the unchanged parent tracer concentration in plasma, $C_{wb}(t)$ is the arterial whole-blood tracer concentration, and $pfp(t)$ is the parent fraction in plasma function.[18,24]

No partial volume recovery correction ($RC = 1$) was applied. The fraction of blood volume (f_{wb}) within myocardial tissue was estimated together with the one-tissue compartment model parameters (K_1, k_2) as follows:

$$C_m(t) = f_{wb} \times C_{wb}(t) + RC \times C_p(t) * K_1 e^{-k_2 t} \quad (3)$$

where * is the mathematical convolution operator.

Regional Heterogeneity—Regional defect scores based on tracer normalized uptake (NUDS) and distribution volume (DVDS) reflect the extent × severity of relative defects, expressed as a percent of the left ventricle.[25] The defect scores were calculated by quantifying tracer uptake or DV in 496 myocardial sectors; those with ≥75% relative to the peak tracer activity were defined as normal and set to equal 100%. The defect score was then calculated as 100% minus the average polar-map value.

Clinical Endpoint

The primary PAREPET endpoint was SCA, including ICD discharge for fast ventricular tachycardia (>240 bpm) or ventricular fibrillation as an equivalent. The secondary endpoint in the competing risks analysis was total cardiac mortality, including both SCA and non-sudden cardiac arrest. Events were arbitrated blindly by 3 board-certified cardiologists.[15]

Statistical Analysis

Continuous variables were represented as mean±SD. Correlations between regional heterogeneity and global scale parameters were performed using a Pearson's Correlation coefficient. A D'Agostino-Pearson omnibus normality test was first performed on the data. For the PET parameters, both regional heterogeneity parameters (NUD score and DV defect score) were normally distributed. For the global scale parameters, DV was normally distributed but RI was not. In figure 2, we used a one-way analysis of variance (ANOVA), or a Kruskal-Wallis test to assess statistical differences in global parameters at increasing severity of regional uptake defect values, where appropriate. The degree of agreement/ disagreement between the PET parameter tertiles was assessed using the weighted kappa. Time-to-endpoint was analyzed using the Kaplan-Meier method and differences between tertiles were assessed by the Log-Rank test. A Cox-proportional hazards regression was also used to assess the association between the HED PET parameters and SCA. A competing risks analysis was performed to simultaneously assess the HED PET parameters associated with SCA and NSCD. In the aforementioned analysis, a multivariate analysis was also performed with global scale values (RI or DV) and the Normalized Uptake Defect Score entered as predictors to identify any independent value of global quantification. Area under (AUC) the receiver operator characteristic (ROC) curve was used to assess the ability of the individual HED PET parameters to discriminate between patients who developed SCA versus those who did not. For this analysis, discrimination was compared at the median follow-up time of 4.2 years. We also evaluate the incremental value of global scale parameters when added to regional defect parameters using the methods of Delong, Delong, and Clarke-Pearson [26]. In the original PAREPET trial, a 4 variable clinical model was created consisting of i) the HED uptake defect score, ii) creatinine, iii) indexed LVEDV, and iv) no ACE/ARB therapy. [15] Stepwise selection was used to generate this multi-variate model to predict time to SCA from PET using the Cox proportional hazard model. From this model, optimized cut points were derived (NU defect score >37% of LV, creatinine >1.49 mg/dL, LVEDVI >99 mL/m^2, and no ACE/ARB therapy). Patients with none of these risk factors had a SCA risk of <1%/year, whereas patients with ≥2 risk factors had a SCA event rate of 11.7%/year. In this clinical model, we scrutinized the ability of the global scale HED parameters to re-classify patients across these event thresholds. The incremental additive value of the global parameters were assessed using the net reclassification index (NRI) and the integrated discrimination improvement (IDI).[27] The IDI evaluates reclassification as a continuous outcome across the spectrum of risk, whereas NRI is defined by prespecified thresholds, chosen *a priori*. P<0.05 was considered statistically significant. Statistical analysis and graphical representation were performed using SAS 9.4 (SAS Institute, NC), and GraphPad Prism 6.0 (GraphPad, La Jolla, CA, USA).

Results:

Patient demographics and characteristics appear in Table 1. Overall patients were optimally treated with 97% on β-blocker therapy, 90% on an ACE or ARB, and 99% receiving either warfarin or antiplatelet therapy. After a median follow-up of 4.2 years (IQR: 2.7-5.3 years) there were 56 cardiac related deaths (n=26 SCA, n=30 non-sudden cardiac death (NSCD)), and 25 non-cardiac related deaths (NCD).

Agreement Between HED Quantification

Four HED quantification methods were performed, two regional heterogeneity defect parameters (NUDS and DVDS) and two global scale parameters (RI and DV). To investigate the agreement between the quantification methods, patients were stratified into tertiles based on their respective regional heterogeneity defect and global scale parameters. There was good to excellent agreement within the global (weighted kappa=0.53 [95%CI 0.43,0.64]) and regional heterogeneity defect (weighted kappa=0.71 [95%CI 0.63,0.79]) quantification values (Table 2). In contrast, there was poor agreement between regional heterogeneity defect and global scale parameters tertiles (weighted kappa 0.16-0.34). Similarly, there were weak linear correlations between the global scale and regional heterogeneity defect parameters (RI: r^2=0.049; DV: r^2=0.082; Figure 2 C,D). Interestingly, for a given regional defect size, there was substantial heterogeneity in global HED DV (Figure 2A) and RI (Figure 2B) values, with no consistent reductions in these parameters until the regional defect size increased above 40% LV ($p<0.05$). Representative polar maps (Figure 3) illustrate this concept. We aimed to investigate whether the global parameters offer any independent, or additive prognostic value.

HED Parameters and Survival

The HED regional defect scores and global scale parameters association with time to the cardiac end points are summarized in Table 3. Only the regional defect parameters were associated with total cardiac mortality ($p<0.05$), whereas both regional defect and global scale parameters were associated with SCA ($p<0.05$). None of the HED parameters were associated with non-sudden cardiac death. Kaplan-Meier curves summarize this data (Figure 4). After adjusting for competing risks, SCA was associated with increased regional defect size, NU (p=0.0025) and DV (p=0.0005), and decreased global scale parameters, DV (p=0.04), RI (p=0.02) as shown in Table 4. However, after statistically controlling for regional defect scores (NUDS), these global scale parameters were no longer significantly associated with SCA in the competing-risk model (Table 4). In the unadjusted competing risk analysis, the effect of each of these HED quantification parameters on probability of SCA, NSCD and non-cardiac death is illustrated in Figure 5.

HED Parameters and SCA Risk prediction

Table 5 and Figure 6 summarize the AUCs for the individual HED quantification methods for predicting SCA. Of these parameters, the regional normalized uptake defect score (NUDS) had the best SCA risk discrimination (AUC 0.74) and had a significantly higher AUC than both global RI (ΔAUC=0.13, p=0.03) and global DV (ΔAUC=0.12, p=0.04). The addition of either global parameter to the regional normalized uptake defect score did not significantly improve the AUC (Table 5). In the original PAREPET trial, a 4-variable clinical model was created consisting of i) the normalized uptake defect score, ii) creatinine, iii) indexed LVEDV, and iv) no ACE/ARB therapy (Table 6). [15] From this model, optimized cut points were derived (NUDS >37% of LV, creatinine >1.49 mg/dL, LVEDVI >99 mL/m^2, and no ACE/ARB therapy). Patients with none of these risk factors had a SCA risk of <1%/year, whereas patients with ≥2 risk factors had a SCA event rate of 11.7%/year. In this clinical model, we scrutinized the ability of the global scale HED parameters to re-classify patients

across these event thresholds. Global Scale RI and DV did not significantly improve the model and appropriately reclassify patients in accordance with their SCA risk (NRI and IDI not significant, Table 7).

Discussion

This study represents the first assessment of both regional heterogeneity and global scale (or intensity) of sympathetic activity measurements for predicting cause-specific mortality from SCA. In this *post hoc* analysis of the PAREPET trial, two regional parameters (NUDS and DVDS) and two global parameters (RI and DV) were investigated. Four major findings were derived in this study. 1) For a given regional defect size, there is substantial variability in global scale quantification values. We further assessed whether there was any independent and additive prognostic value in these global scale parameters. 2) In a competing-risk analysis, both global scale and regional heterogeneity parameters were associated with SCA risk, but not non-sudden cardiac death and non-cardiac death. 3) Global scale parameters have inferior SCA risk discrimination as compared to regional parameters and yield no additive or independent prognostic value. 4) Overall, there were no differences between uptake versus DV defect scores with respect to SCA risk prediction. These results have widespread implications for future cardiac sympathetic HED analysis and imaging protocols. Taken together we demonstrate that SCA risk stratification is sufficiently predicted with conventional HED uptake defect scores, whereas other more sophisticated quantification measures of regional heterogeneity (DV defect score) and global scale (RI and DV) may not be required for risk stratification.

Relationship Between Global and Regional Sympathetic Activity

Our results corroborate previous findings of a strong correlation between global RI and DV parameters.[23] The poor correlation between global and regional parameters is novel and arises from substantial heterogeneity in global tracer uptake and retention. As a result, for a given regional defect size, there can be either global preservation or downregulation of tracer uptake. Alterations in HED uptake can arise from both anatomical and functional properties of the cardiac SNS.[28] Indeed, it is not possible to differentiate the relative contribution of dysinnervation or neuronal stunning from denervation (true loss of sympathetic nerves) using a single tracer approach.[28] Preclinical studies indicate that sympathetic nerve function is particularly susceptible to ischemia, whereas denervation and a loss of sympathetic nerves arise in the infarct and peri-infarct risk region. In addition, sympathetic nerve sprouting occurs at the border between infarcted and normal tissue and this hyperinnervation carries significant arrhythmogenic risk[29]. All of these contribute to inhomogeneity in sympathetic innervation and the resulting substrate for lethal ventricular arrhythmias.[30,31] In contrast, global reductions in tracer uptake are affected by these regional alterations as well as elevated SNS tone, high systemic norephinephrine (NE) or a global reduction in Uptake1 (NE transporter).[28,32,33] Mechanistically, the distinction between neuronal stunning and denervation may be clinically important, as the former may be reversible and less likely to induce nerve sprouting as compared to denervated myocardium.

Competing Risks Analysis

A recent competing risk analysis of the PAREPET trial identified PET and clinical variables associated with cause-specific cardiac mortality. In this analysis, SCA was correlated with greater regional HED defect score, lack of ACE/ARC therapy, elevated BNP and larger LVEDV index.[13] The denervation volume was not associated with non-sudden cardiac death.[13] The present analysis extends these findings by comparing regional defect and global scale HED parameters in the competing risk analysis. This analysis enables the assessment of the independent components of cardiac mortality, namely SCA and NSCD. In our analysis both regional and global HED parameters were associated with cause-specific mortality from SCA, but not NSCD or NCD. However, after adjusting for regional defect size, the global RI and DV were not associated with SCA, indicating that global scale parameters offer no independent prognostic information.

SCA Risk Discrimination

In the original PAREPET trial, global RI values were not statistically different in patients that had an arrhythmic event or ICD equivalent.[15] These results were corroborated in a separate HED imaging study of ischemic cardiomyopathy patients (EF<35%).[6] In the latter study, patients underwent an electrophysiological study (EPS) after ICD implantation. Global RI values were not different in patients with inducible ventricular arrhythmias (RI EPS positive 2.41 versus EPS negative 2.81, p=0.07). However, in both of these analysis regional and global HED quantification SCA risk prediction were not formally compared. We demonstrated that the global scale parameters have inferior SCA risk discrimination as compared to the regional uptake defect score used in the PAREPET trial. Previous studies have demonstrated that inhomogeneity in myocardial sympathetic innervation results in a substrate at particular risk of arrhythmogenesis.[34] In myocardial infarction, this arises from regional sympathetic denervation hypersensitivity and spatial alterations in action potential duration that may promote re-entrant arrhythmias.[35] Inhomogeneity can also arise in viable dysfunctional myocardium as a result of alterations in sympathetic nerve density, nerve sprouting and alterations in myocardial beta-receptor density and function.[30,36-38] There are several potential explanations why imaging this heterogeneity may be superior to assessing it indirectly with global indices of 11-CHED uptake in our analysis. First, heterogeneity in sympathetic activation was assessed by comparing reductions in 11-CHED relative to normal regions in each individual patient. In contrast, global alterations in 11-CHED uptake reflect reductions in both dysinnervated regions as well as altered uptake in normal myocardium. Uptake in normal myocardium could vary with myocardial sympathetic tone, circulating catecholamine levels and potentially pharmacological interventions that would modulate neurohormonal activation.[39] As a result, the same regional defect could have variable levels of global uptake in normal myocardium. Furthermore, while our analysis compared global indices to regional indices in individual patients, application of a global index clinically would require identification of a specific cut point and/or comparison to a normal data set. The variability in uptake among individuals may require a greater difference in global uptake and result in a further deterioration in predictive value. Based on these considerations, we believe that quantifying regional defects offers advantages over global indices using PET 11-CHED. Whether this extends to other norepinephrine analogs and imaging platforms will require further study.

The global scale parameters also offered no incremental discrimination as compared to the regional defect parameters alone. In a recent test-retest analysis, we demonstrated that HED regional defect parameters also have better reproducibility than global scale parameters.[23] Together, these results suggest regional defect parameters may be the optimal approach for routine clinical SCA risk prediction in patients with ischemic cardiomyopathy.

Comparison to Previous Studies

The present study is the first to directly compare the SCA discrimination of various HED PET imaging parameters. Numerous tracers and modalities have been studied in the context of cardiac denervation, notably MIBG with SPECT imaging. A number of studies have examined global cardiac sympathetic innervation using the tracer MIBG to predict cardiovascular outcomes in heart failure patients, but there also remains equipoise regarding the optimal parameters to predict cardiovascular risk. While global indices of tracer quantification including the heart-to-mediastinum ratio and MIBG washout rate have been studied, quantitative analysis of regional defect size with SPECT has been challenging.[12] The lower detection sensitivity and resolution of SPECT imaging compared to PET renders it difficult to separate regional defects from global levels of innervation.[40] The ADMIRE-HF trial enrolled 961 participants with an LVEF ≤ 35% and NYHA Class II/III symptoms and examined a composite outcome of heart failure progression, potentially life-threatening arrhythmias and cardiac death.[12] This large study included ischemic and nonischemic cardiomyopathy patients and found the H/M ratio (similar to the global scale RI in our study) to be predictive of the composite primary endpoint. Another study (n=116), in patients with an ICD indication for both primary and secondary prevention, examined the MIBG H/M ratio, washout rate, and defect score, and found only the defect score by SPECT was predictive of ventricular arrhythmias.[10] This is consistent with our analysis of quantifying regional defect score and the primary endpoint of SCA. While quantifying defect volume with SPECT is challenging, technical advances such as CZT cameras may allow this in the future.

In a *post-hoc* analysis of the ADMIRE-HF data, Travin *et al.* proposed a ‘bell-shaped’ relationship between regional MIBG defect scores (regional parameter) and arrhythmic events, such that patients with ‘intermediate-range’ defects had the highest proportion of events.[41] This hypothesis has been subsequently supported by two separate research groups. In these studies, Verschure *et al.* and Nakajima *et al.* similarly revealed a bell-shaped between MIBG H/M ratio (global scale parameter) and combined arrhythmic death and appropriate ICD discharge.[42,43] To our knowledge, no such relationship has been observed for HED. In the present manuscript, Figure 4B visually hinted at such a relationship with the relationship between RI (global scale parameter) and SCA. However, there was no statistical difference between the Low and Intermediate Tertiles. In Supplemental Figure 1, we further explored the relationship between regional heterogeneity or global scale parameters and SCA on a continuous scale. Most importantly, the regional defect scores based on HED Uptake (A) or Distribution Volume (B) showed no hint of a bimodal distribution or ‘bell-shaped’ risk profile, contrary to the MIBG SPECT data. For the global scale parameters (C, D), specifically exploring the relationship between SCA-free survival and the retention index, a few patients with relatively low values of the RI (C) appear to show a slight

improvement in survival (see red arrow), but this subsequently decreases again as the RI approaches zero. Given the very small sample size in this range (only 2 patients with RI values < 2%/min), it seems most likely that this effect is due to normal heterogeneity in the data and not a real physiological effect.

Study Limitations

While appropriate ICD therapy for VF or VT at rates of 240 BPM and faster were used as a surrogate for aborted arrhythmic death, ventricular arrhythmias at slower rates were not considered as a primary end-point. Currently there is no consensus regarding which classification of ICD discharge represents the most appropriate definition. Available evidence suggests that using the definition of the present study, the rate of ICD discharge is approximately similar to the difference in mortality rate in clinical trials comparing patients receiving a primary prevention ICD with coronary artery disease versus a medically treated population. [44] A broader analysis of ventricular arrhythmias in the PAREPET trial demonstrated that the HED defect size did not predict slower ventricular arrhythmias and the prognostic impact of HED for VF and fast VT remained.[45] It is important to note that while these data have important imaging implications for patients with ischemic cardiomyopathy, the global data findings cannot be applied to patients with non-ischemic cardiomyopathy as they were not part of the present cohort.

Clinical Implications

The findings of this study may have implications for broader implementation of imaging myocardial sympathetic innervation. Current HED quantification methods have varying degrees of sophistication. Regional HED activity uptake quantification capabilities are likely available with most commercial PET software. In contrast, parametric imaging of distribution volume, which also requires kinetic modeling and long image acquisition times, may only be available to academic institutions that have access to compartmental analysis. A key finding of our study was that absolute global scale values such as RI and DV yield no independent or additive benefit clinical use in distinguishing SCA risk. This greatly simplifies future PET innervation imaging for predicting clinically meaningful outcomes and should facilitate translation into clinical care as fluorinated norepinephrine analogs become available to assess regional inhomogeneity in sympathetic innervation with PET.

Supplementary Material

Refer to Web version on PubMed Central for supplementary material.

Acknowledgments

Funding: This study was supported in part by research grants-in-aid (Heart and Stroke Foundation of Ontario T6426 and NA7158), by the IMAGE–Heart Failure team grant (Canadian Institutes of Health Research CIF99470), the National Heart and Blood Institute (HL-76252 and HL-130266), National Center for Advancing Translational Sciences (UL1TR001412), and the Advanced Imaging in Heart Failure grant (Ontario Research Fund ORF-RE-07-029). RSB holds a Tier 1 uOttawa Research Chair in Cardiovascular Research and is supported by the Ottawa Heart Institute Vered Chair in Cardiology. JGEZ is an MD/PhD student supported in part by the Vanier Graduate Scholarship and the University of Ottawa.

Abbreviations

DV	Distribution Volume
DVDS	Distribution Volume Defect Score
HED	[^{11}C]*meta*-hydroxyephedrine
ICD	Implantable Cardioverter-Defibrillator
NCD	Non-Cardiac Death
NSCD	Non-Sudden Cardiac Death
NUDS	Normalized Uptake Defect Score
RI	Retention Index
SCA	Sudden Cardiac Arrest
SNS	Sympathetic Nervous System

References

1. Myerburg RJ, Kessler KM, Castellanos A. Sudden cardiac death: epidemiology, transient risk, and intervention assessment. Ann Intern Med. 1993;119:1187–1197. [PubMed: 8239250]
2. Wannamethee G, Shaper AG, Macfarlane PW, Walker M. Risk factors for sudden cardiac death in middle-aged British men. Circulation. 1995;91:1749–1756. [PubMed: 7882483]
3. Bennett M, Parkash R, Nery P, Sénéchal M, Mondesert B, Birnie D, Sterns LD, Rinne C, Exner D, Philippon F, Campbell D, Cox J, Dorian P, Essebag V, Krahn A, Manlucu J, Molin F, Slawnych M, Talajic M. Canadian Cardiovascular Society/Canadian Heart Rhythm Society 2016 Implantable Cardioverter-Defibrillator Guidelines. Can J Cardiol. 2017;33:174–188. [PubMed: 28034580]
4. Exner DV, Kavanagh KM, Slawnych MP, Mitchell LB, Ramadan D, Aggarwal SG, Noullett C, Van Schaik A, Mitchell RT, Shibata MA, Gulamhussein S, McMeekin J, Tymchak W, Schnell G, Gillis AM, Sheldon RS, Fick GH, Duff HJ, REFINE Investigators. Noninvasive risk assessment early after a myocardial infarction the REFINE study. J Am Coll Cardiol. 2007;50:2275–2284. [PubMed: 18068035]
5. Moss AJ, Greenberg H, Case RB, Zareba W, Hall WJ, Brown MW, Daubert JP, McNitt S, Andrews ML, Elkin AD, Multicenter Automatic Defibrillator Implantation Trial-II (MADIT-II) Research Group. Long-term clinical course of patients after termination of ventricular tachyarrhythmia by an implanted defibrillator. Circulation. 2004;110:3760–3765. [PubMed: 15583079]
6. Rijnierse MT, Allaart CP, de Haan S, Harms HJ, Huisman MC, Beek AM, Lammertsma AA, van Rossum AC, Knaapen P. Non-invasive imaging to identify susceptibility for ventricular arrhythmias in ischaemic left ventricular dysfunction. Heart. 2016;102:832–840. [PubMed: 26843532]
7. Huikuri HV, Castellanos A, Myerburg RJ. Sudden Death Due to Cardiac Arrhythmias. N Engl J Med. 2001;345:1473–1482. [PubMed: 11794197]
8. Nishisato K, Hashimoto A, Nakata T, Doi T, Yamamoto H, Nagahara D, Shimoshige S, Yuda S, Tsuchihashi K, Shimamoto K. Impaired Cardiac Sympathetic Innervation and Myocardial Perfusion Are Related to Lethal Arrhythmia: Quantification of Cardiac Tracers in Patients with ICDs. J Nucl Med. 2010;51:1241–1249. [PubMed: 20679471]
9. Bax JJ, Kraft O, Buxton AE, Fjeld JG, Parizek P, Agostini D, Knuuti J, Flotats A, Arrighi J, Muxi A, Alibelli M-J, Banerjee G, Jacobson AF. 123I-mIBG Scintigraphy to Predict Inducibility of Ventricular Arrhythmias on Cardiac Electrophysiology Testing: A Prospective Multicenter Pilot Study. Circ Cardiovasc Imaging. 2008;1:131–140. [PubMed: 19808530]

10. Boogers MJ, Borleffs CJW, Henneman MM, van Bommel RJ, van Ramshorst J, Boersma E, Dibbets-Schneider P, Stokkel MP, van der Wall EE, Schalij MJ, Bax JJ. Cardiac sympathetic denervation assessed with 123-iodine metaiodobenzylguanidine imaging predicts ventricular arrhythmias in implantable cardioverter-defibrillator patients. J Am Coll Cardiol. 2010;55:2769–2777. [PubMed: 20538172]
11. Kasama S, Toyama T, Kaneko Y, Iwasaki T, Sumino H, Kumakura H, Minami K, Ichikawa S, Matsumoto N, Sato Y, Kurabayashi M. Relationship between late ventricular potentials and myocardial 123I-metaiodobenzylguanidine scintigraphy in patients with dilated cardiomyopathy with mild to moderate heart failure: results of a prospective study of sudden death events. Eur J Nucl Med Mol Imaging. 2012;39:1056–1064. [PubMed: 22415599]
12. Jacobson AF, Senior R, Cerqueira MD, Wong ND, Thomas GS, Lopez VA, Agostini D, Weiland F, Chandna H, Narula J. Myocardial Iodine-123 Meta-Iodobenzylguanidine Imaging and Cardiac Events in Heart Failure. J Am Coll Cardiol. 2010;55:2212–2221. [PubMed: 20188504]
13. Fallavollita JA, Dare JD, Carter RL, Baldwa S, Canty JM. Denervated Myocardium Is Preferentially Associated With Sudden Cardiac Arrest in Ischemic Cardiomyopathy: A Pilot Competing Risks Analysis of Cause-Specific Mortality. Circ Cardiovasc Imaging. 2017;10.
14. Imanli H, Ume KL, Jeudy J, Bob-Manuel T, Smith MF, Chen W, Abdulghani M, Ghzally Y, Mahat JB, Itah R, Restrepo A, See VY, Shorofsky S, Dilsizian V, Dickfeld T. Ventricular Tachycardia (VT) Substrate Characteristics: Insights from Multimodality Structural and Functional Imaging of the VT Substrate Using Cardiac MRI Scar, 123 I-Metaiodobenzylguanidine SPECT Innervation, and Bipolar Voltage. J Nucl Med. 2019;60:79–85. [PubMed: 29959218]
15. Fallavollita JA, Heavey BM, Luisi AJ, Michalek SM, Baldwa S, Mashtare TL, Hutson AD, Haka MS, Sajjad M, Cimato TR. Regional myocardial sympathetic denervation predicts the risk of sudden cardiac arrest in ischemic cardiomyopathy. J Am Coll Cardiol. 2014;63:141–149. [PubMed: 24076296]
16. Münch G, Nguyen NTB, Nekolla S, Ziegler S, Muzik O, Chakraborty P, Wieland DM, Schwaiger M. Evaluation of sympathetic nerve terminals with [11C] epinephrine and [11C] hydroxyephedrine and positron emission tomography. Circulation. 2000;101:516–523. [PubMed: 10662749]
17. Raffel DM, Chen W, Sherman PS, Gildersleeve DL, Jung Y-W. Dependence of cardiac 11C-meta-hydroxyephedrine retention on norepinephrine transporter density. J Nucl Med. 2006;47:1490–1496. [PubMed: 16954558]
18. DeGrado TR, Hutchins GD, Toorongian SA, Wieland DM, Schwaiger M. Myocardial kinetics of carbon-11-meta-hydroxyephedrine: retention mechanisms and effects of norepinephrine. J Nucl Med. 1993;34:1287–1293. [PubMed: 8326386]
19. Fricke E, Eckert S, Dongas A, Fricke H, Preuss R, Lindner O, Horstkotte D, Burchert W. Myocardial sympathetic innervation in patients with symptomatic coronary artery disease: Follow-up after 1 year with neurostimulation. J Nucl Med. 2008;49:1458–1464. [PubMed: 18703600]
20. Harms HJ, de Haan S, Knaapen P, Allaart CP, Rijnierse MT, Schuit RC, Windhorst AD, Lammertsma AA, Huisman MC, Lubberink M. Quantification of [11 C]-meta-hydroxyephedrine uptake in human myocardium. EJNMMI Res. 2014;4:52. [PubMed: 26116116]
21. Fallavollita JA, Luisi AJ, Michalek SM, Valverde AM, deKemp RA, Haka MS, Hutson AD, Canty JM. Prediction of arrhythmic events with positron emission tomography: PAREPET study design and methods. Contemp Clin Trials. 2006;27:374–388. [PubMed: 16647885]
22. Innis RB, Cunningham VJ, Delforge J, Fujita M, Gjedde A, Gunn RN, Holden J, Houle S, Huang S-C, Ichise M. Consensus nomenclature for in vivo imaging of reversibly binding radioligands. J Cereb Blood Flow Metab. 2007;27:1533–1539. [PubMed: 17519979]
23. Wu KY, Zelt JGE, Wang T, Dinculescu V, Miner R, Lapierre C, Kaps N, Lavallee A, Renaud JM, Thackeray J, Mielniczuk LM, Chen S-Y, Burwash IG, DaSilva JN, Beanlands RSB, deKemp RA. Reliable quantification of myocardial sympathetic innervation and regional denervation using [11C]meta-hydroxyephedrine PET. Eur J Nucl Med Mol Imaging. 2019;
24. Thackeray JT, Beanlands RS, DaSilva JN. Presence of specific 11C-meta-hydroxyephedrine retention in heart, lung, pancreas, and brown adipose tissue. J Nucl Med. 2007;48:1733–1740. [PubMed: 17873125]

25. Wang Jean Z., Moody Jonathan B., Kaps Nicole, Britt Deron, Lavallee Aaryn, Renaud Jennifer M., Zelt Jason G. E., Wu Kai Yi, Beanlands Rob S., Fallavollita James A., Canty John M., deKemp Robert A.. Reproducible Quantification of Regional Sympathetic Denervation with [11C]meta-Hydroxyephedrine PET Imaging. J Nucl Cardiol. 2020;
26. DeLong ER, DeLong DM, Clarke-Pearson DL. Comparing the areas under two or more correlated receiver operating characteristic curves: a nonparametric approach. Biometrics. 1988;44:837–845. [PubMed: 3203132]
27. Pencina MJ, D'Agostino RB, D'Agostino RB, Vasan RS. Evaluating the added predictive ability of a new marker: from area under the ROC curve to reclassification and beyond. Stat Med. 2008;27:157–172; discussion 207-212. [PubMed: 17569110]
28. Zelt JGE, deKemp RA, Rotstein BH, Nair GM, Narula J, Ahmadi A, Beanlands RS, Mielniczuk LM. Nuclear Imaging of the Cardiac Sympathetic Nervous System: A Disease-Specific Interpretation in Heart Failure. JACC Cardiovasc Imaging. 2019;
29. Cao J-M, Fishbein MC, Han JB, Lai WW, Lai AC, Wu T-J, Czer L, Wolf PL, Denton TA, Shintaku IP, others. Relationship between regional cardiac hyperinnervation and ventricular arrhythmia. Circulation. 2000;101:1960–1969. [PubMed: 10779463]
30. Pizzuto MF, Valverde AM, Heavey BM, Banas MD, Michelakis N, Suzuki G, Fallavollita JA, Canty JM. Brief sympathetic activation precedes the development of ventricular tachycardia and ventricular fibrillation in hibernating myocardium. J Electrocardiol. 2006;39:S140–S145. [PubMed: 16919670]
31. Fukuda K, Kanazawa H, Aizawa Y, Ardell JL, Shivkumar K. Cardiac Innervation and Sudden Cardiac Death. Circ Res. 2015;116:2005–2019. [PubMed: 26044253]
32. Thackeray JT, Renaud JM, Kordos M, Klein R, deKemp RA, Beanlands RSB, DaSilva JN. Test–retest repeatability of quantitative cardiac 11C-meta-hydroxyephedrine measurements in rats by small animal positron emission tomography. Nucl Med Biol. 2013;40:676–681. [PubMed: 23664690]
33. Ungerer M, Hartmann F, Karoglan M, Chlistalla A, Ziegler S, Richardt G, Overbeck M, Meisner H, Schomig A, Schwaiger M. Regional In Vivo and In Vitro Characterization of Autonomic Innervation in Cardiomyopathic Human Heart. Circulation. 1998;97:174–180. [PubMed: 9445170]
34. Fallavollita JA, Canty JM. Dysinnervated but viable myocardium in ischemic heart disease. J Nucl Cardiol. 2010;17:1107–1115. [PubMed: 20857351]
35. Inoue H, Zipes DP. Time course of denervation of efferent sympathetic and vagal nerves after occlusion of the coronary artery in the canine heart. Circ Res. 1988;62:1111–1120. [PubMed: 3383360]
36. Iyer VS, Canty JM. Regional Desensitization of β-Adrenergic Receptor Signaling in Swine With Chronic Hibernating Myocardium. Circ Res. 2005;97:789–795. [PubMed: 16141409]
37. Ovchinnikov V, Suzuki G, Canty JM, Fallavollita JA. Blunted functional responses to pre- and postjunctional sympathetic stimulation in hibernating myocardium. Am J Physiol Heart Circ Physiol. 2005;289:H1719–1728. [PubMed: 15923318]
38. Fernandez SF, Ovchinnikov V, Canty JM, Fallavollita JA. Hibernating myocardium results in partial sympathetic denervation and nerve sprouting. Am J Physiol-Heart Circ Physiol. 2013;304:H318–H327. [PubMed: 23125211]
39. Chizzola PR, Gonçalves de Freitas HF, Marinho NVS, Mansur JA, Meneghetti JC, Bocchi EA. The effect of β-adrenergic receptor antagonism in cardiac sympathetic neuronal remodeling in patients with heart failure. Int J Cardiol. 2006;106:29–34. [PubMed: 16321662]
40. Boschi S, Lodi F, Boschi L, Nanni C, Chondrogiannis S, Colletti PM, Rubello D, Fanti S. 11C-Meta-Hydroxyephedrine: A Promising PET Radiopharmaceutical for Imaging the Sympathetic Nervous System. Clin Nucl Med. 2015;40:e96–e103. [PubMed: 24999701]
41. Travin MI, Henzlova MJ, van Eck-Smit BLF, Jain D, Carrió I, Folks RD, Garcia EV, Jacobson AF, Verberne HJ. Assessment of 123I-mIBG and 99mTc-tetrofosmin single-photon emission computed tomographic images for the prediction of arrhythmic events in patients with ischemic heart failure: Intermediate severity innervation defects are associated with higher arrhythmic risk. J Nucl Cardiol. 2017;24:377–391. [PubMed: 26791866]

42. Verschure DO, de Groot JR, Mirzaei S, Gheysens O, Nakajima K, van Eck-Smit BLF, Aernout Somsen G, Verberne HJ. Cardiac 123 I- m IBG scintigraphy is associated with freedom of appropriate ICD therapy in stable chronic heart failure patients. Int J Cardiol. 2017;248:403–408. [PubMed: 28847545]

43. Nakajima K, Nakata T, Doi T, Tada H, Maruyama K. Machine learning-based risk model using 123I-metaiodobenzylguanidine to differentially predict modes of cardiac death in heart failure. J Nucl Cardiol [Internet]. 2020 [cited 2021 Feb 2];Available from: http://link.springer.com/10.1007/s12350-020-02173-6

44. Moss AJ, Zareba W, Hall WJ, Klein H, Wilber DJ, Cannom DS, Daubert JP, Higgins SL, Brown MW, Andrews ML. Prophylactic Implantation of a Defibrillator in Patients with Myocardial Infarction and Reduced Ejection Fraction. N Engl J Med. 2002;346:877–883. [PubMed: 11907286]

45. Singh V, Malhotra S, Canty J, Fallavollita J. The Volume of Denervated Myocardium Predicts Sudden Cardiac Death (SCD) and ICD Therapies for VF but not ICD Therapies for Slower Ventricular Tachyarrhythmia (VT): An Analysis of the Prediction of Arrhythmic Events with Positron Emission Tomography (PAREPET) Study. J Am Coll Cardiol. 2018;71.

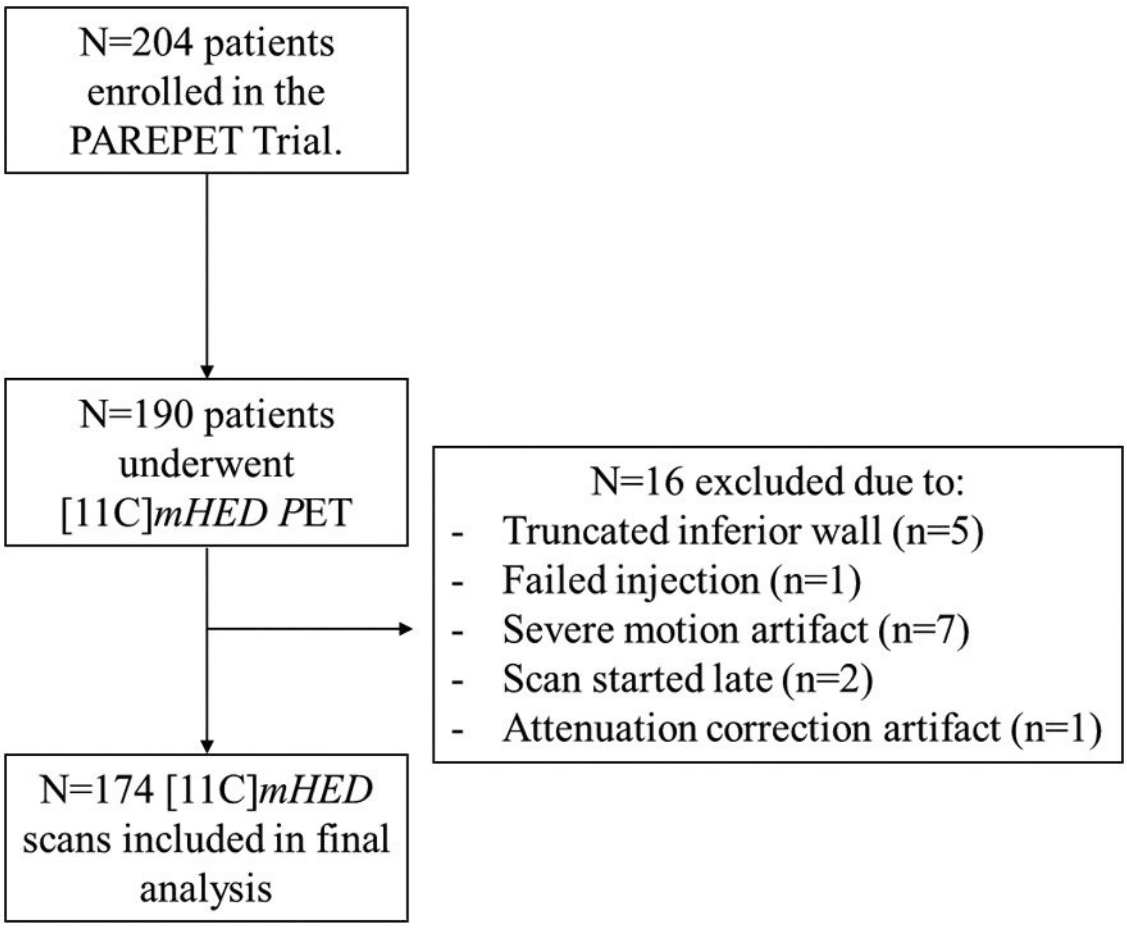

Figure 1.
Flow diagram of patient inclusion/exclusion.

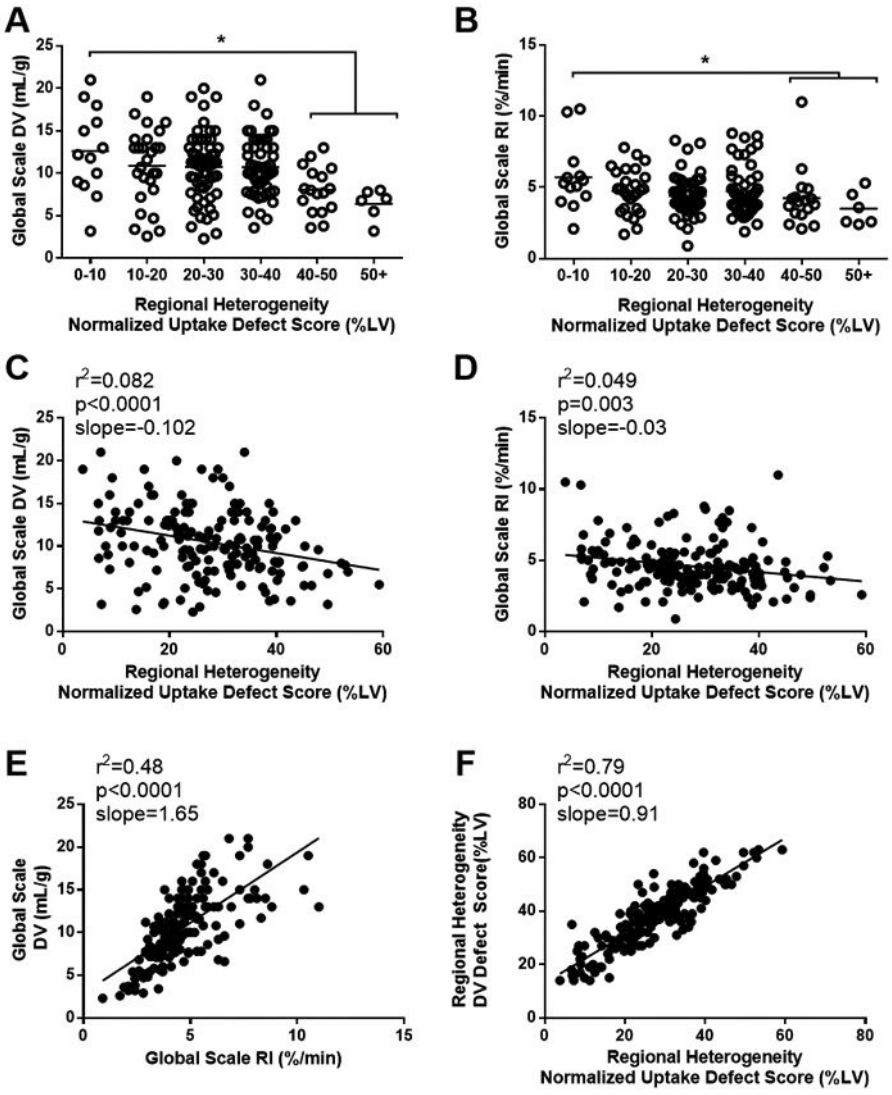

Figure 2.

Relationship between regional heterogeneity and global scale [11C]HED PET parameters. For a given regional heterogeneity defect, patients display a range of global DV (A) and global RI (B) values. Correlations between the regional normalized uptake defect score (used in the PARREPET trial) and global scale parameters displayed (C,D). Excellent correlations were observed within global scale (E) and regional defect (F) [11C]HED PET parameters. DV, distribution volume; RI, retention index; LV, left ventricle.

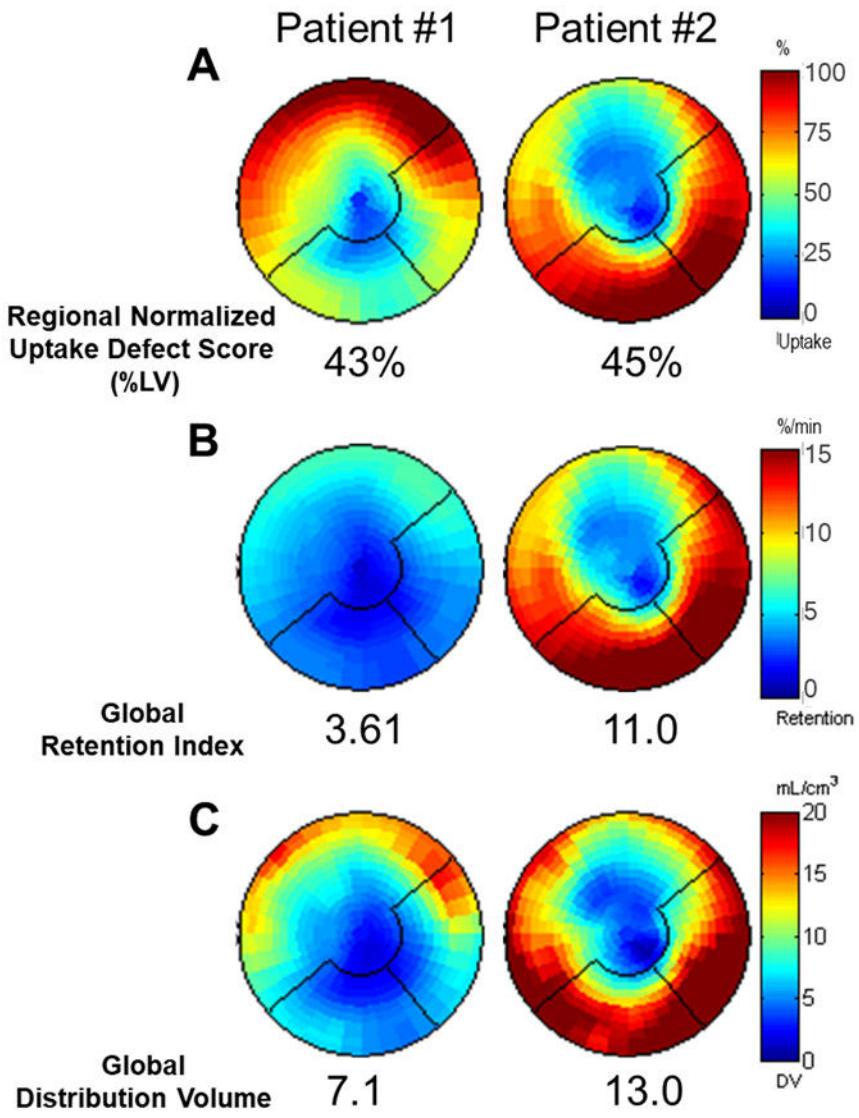

Figure 3.

Polar maps of regional normalized uptake defect score (A), and global scale retention (B) and distribution volume (C) for two patients with similar regional defect scores but differing global RI and DV scores.

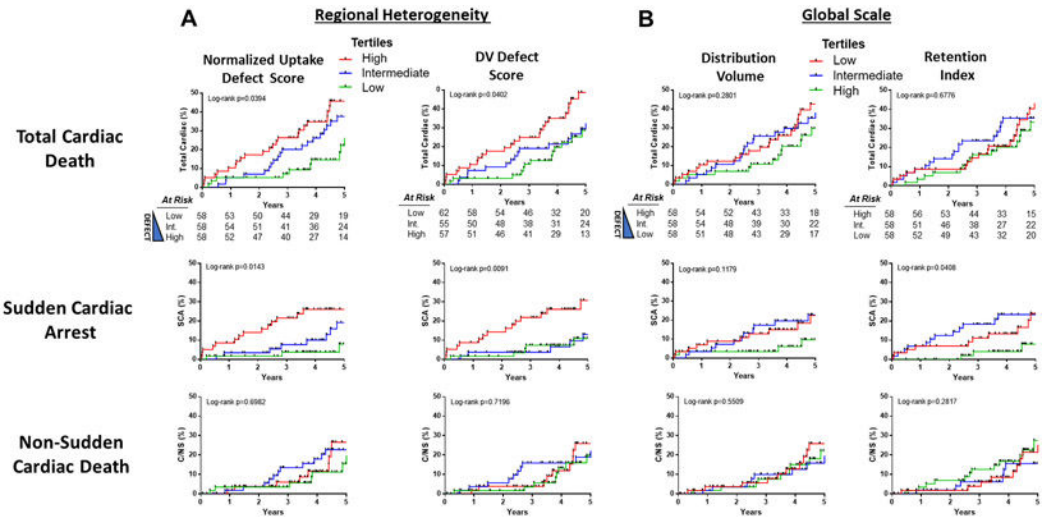

Figure 4.

Kaplan-Meier curves show the incidence of cardiac endpoints for tertiles of regional heterogeneity (A) and global scale (B) [11C]HED quantification methods. Note that the coloring of the tertiles for the global scale parameters (B) is reversed to correspond with the theoretical risk. For the regional defect parameters, the low (green) and high (red) tertiles for Regional Normalized Uptake Defect Score (low: <22.87%, high ≥32.6%) and DV Defect Score (low: <35%, high ≥43%) are shown. Similarly, for the global scale parameters, the low (red) and high (green) tertiles for DV (Low: <8.7mL/g, High: ≥12.2 mL/g) and RI (Low: <3.84 %/min, High: ≥4.85%/min). Corresponding P values for the univariate analysis using continuous variables are in Table 3. SCA, sudden cardiac arrest; C/NS, non-sudden cardiac death.

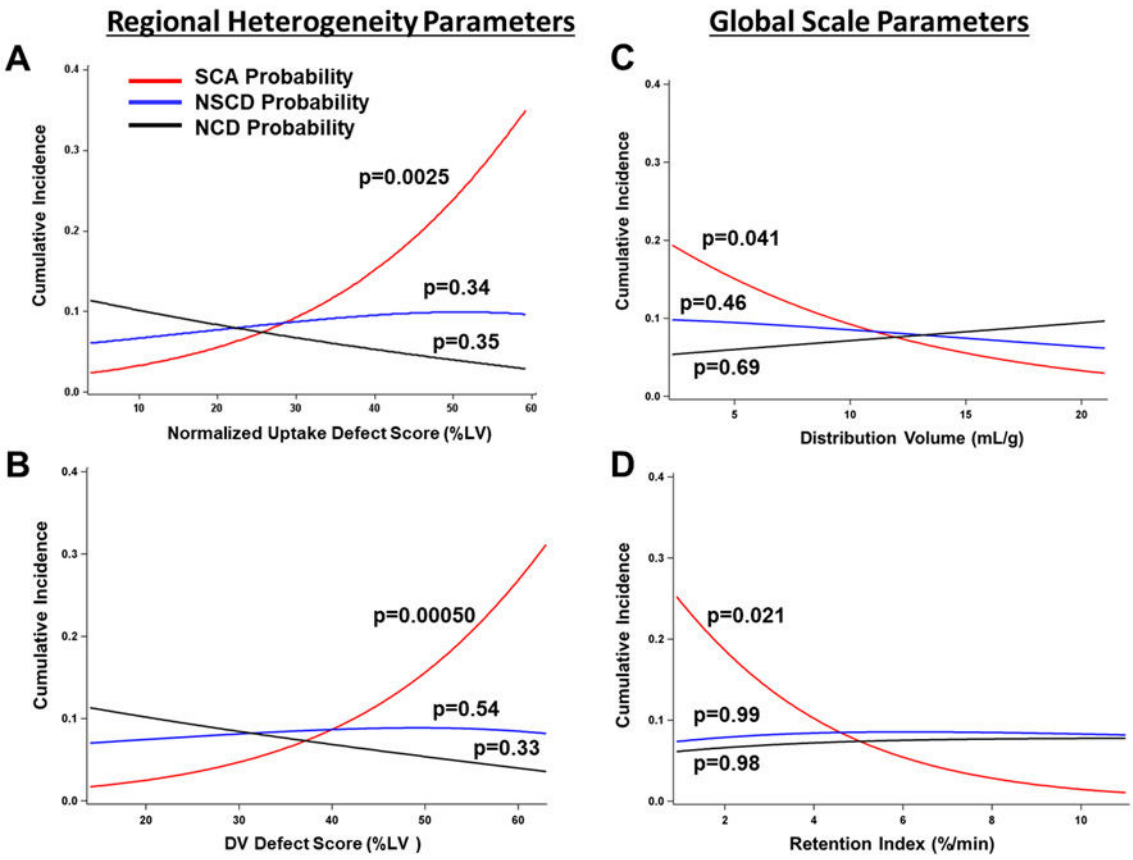

Figure 5.

Estimated event rates from the competing risk analysis for HED PET regional defect and global scale quantification. P values are derived from the competing-risk analysis in Table 4. Figure illustrates the anticipated effect of each HED quantification parameter on SCA (red line), non-sudden cardiac arrest (blue line) and non-cardiac death (black line) within the follow-up period. All HED quantification parameters were associated with SCA after adjusting for competing risks. The effect of each PET parameter was assessed individually. LV, left ventricle; SCA, sudden cardiac arrest; NSCD, non-sudden cardiac death; NCD, non-cardiac death.

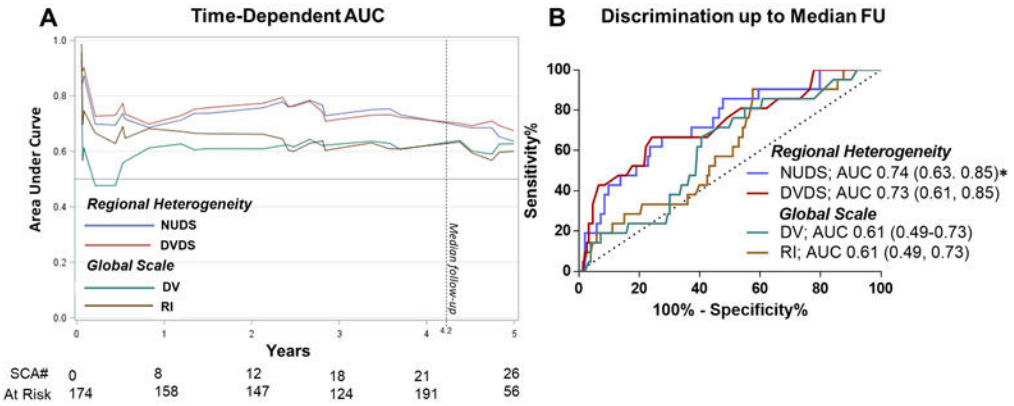

Figure 6.

Comparison of Regional Heterogeneity and Global Scale [11C[HED PET parameters for SCA risk discrimination. Time-dependent AUC illustrate discrimination over time (A). PET parameters were compared up to the median follow-up (4.2years). ROC curve comparison for regional defect and global scale parameters up to median follow-up (B). Corresponding P values are displayed in Table 5. * AUC superior than both global scale parameters, $p<0.05$.

Table 1.

Patient Characteristics

Variables (n=174)	Average
Demographics	
Age (years)	67.6 ±11.6
Sex (male)	156 (90%)
BMI (kg/m^2)	28.7 ± 5.1
Diabetes mellitus	82 (47%)
Resting Heart Rate (bpm)	65 ± 12
Rate/Pressure Product (per 100 bpm/ mm Hg)	8473 ± 2294
No ACE/ARB Therapy	18 (10%)
β-blocker Therapy	168 (97%)
Warfarin	69 (40%)
Antiplatelet (ASA or Clopidogrel)	153 (89%)
Digoxin	67 (39%)
Echocardiographic and Electrocardiographic Variables	
Ejection Fraction (%)	27.6 ± 8.9
LV End Diastolic Volume Index (mL/m^2)	87.1 ± 29.1
LV End Systolic Volume Index (mL/m^2)	63.9 ± 25.5
LA Volume Index (mL/m^2)	41.9 ± 15.7
LV Mass Index (g/m^2)	152.1 ± 47.5
QRS Duration (ms)	136.7 ± 35.5
Laboratory Values	
Creatinine (mg/dL)	1.43 ± 0.9
B-type natriuretic peptide, ng/L	423.1 ±455.8
Hematocrit (%)	40.6 ± 4.9
[11C]HED PET Quantification	
Global Scale Parameters	
Retention Index (%/min)	4.6 ± 1.7
Distribution Volume (mL/g)	10.5 ± 4.0
Regional Heterogeneity Parameters (%LV)	

Variables (n=174)	Average
Normalized Uptake Defect Score	27.5 ± 11.1
Distribution Volume Defect Score	38.0 ±11.4

BMI, Body mass index; ACE, Angiotensin-converting enzyme; ARB, Angiotensin II Receptor Blocker; ASA, Acetylsalicylic acid; LV, Left ventricle; LA, Left Atrial;

Table 2:

Agreement Between PET Parameter Tertiles

Comparison			Weighted Kappa	95% CI
NUDS	vs	DVDS	0.71	0.63, 0.79
	vs	DV Global	0.24	0.12, 0.35
	vs	RI Global	0.16	0.04, 0.28
DVDS	vs	DV Global	0.34	0.22, 0.45
	vs	RI Global	0.21	0.09, 0.33
DV Global	vs	RI Global	0.53	0.43, 0.64

DV, Distribution volume; DVDS, DV Defect Score; NUDS, Normalized Uptake Defect Score; RI, Retention index; CI, Confidence interval.

Table 3:

Univariate Associates with Cardiac Endpoints

PET Variable	Total Cardiac		Sudden Cardiac Arrest		Non-Sudden Cardiac Death		Non-Cardiac Death	
	Hazard Ratio	*p*-Value	Hazard Ratio	*p*-Value	Hazard Ratio	*p*-Value	Hazard Ratio	*p*-Value
Regional Heterogeneity (per 1% of LV)								
NUDS	1.035	0.0053*	1.055	0.0024*	1.016	0.34	0.98	0.35
DVDS	1.035	0.0057*	1.066	0.0008*	1.010	0.54	0.98	0.33
Global Scale (per 1 unit)								
Distribution Volume	0.93	0.057	0.90	0.047*	0.97	0.46	1.02	0.69
Retention Index	0.86	0.12	0.72	0.033*	0.98	0.86	0.99	0.98

NUDS, Normalized Uptake Defect Score; DVDS, DV Defect Score.

Table 4:

Competing Risk Model for SCA vs Non-Sudden Cardiac Death and Non-Cardiac Death.

Variable	Sudden Cardiac Arrest			Non-Sudden Cardiac Death			Non-Cardiac Death		
	Hazard Ratio	95%CI	*p*-Value	Hazard Ratio	95%CI	*p*-Value	Hazard Ratio	95%CI	*p*-Value
Regional Heterogeneity (per 1% LV)									
NUDS	1.055	1.019, 1.092	0.0025*	1.016	0.983, 1.051	0.3398	0.982	0.946, 1.019	0.3451
DVDS	1.066	1.027, 1.106	0.0005*	1.010	0.978, 1.044	0.5421	0.983	0.948, 1.018	0.3347
Global Scale (per 1 unit)									
Distribution Volume	0.897	0.806, 0.998	0.041*	0.964	0.875, 1.063	0.4620	1.022	0.919, 1.136	0.6922
Retention Index	0.713	0.524, 0.972	0.021*	0.980	0.783, 1.228	0.8624	0.997	0.773, 1.286	0.9823
Multivariable Model									
Model A									
NUDS	1.048	1.011, 1.086	0.010*	-	-	-	-	-	-
Global Scale RI	0.788	0.578, 0.788	0.134	-	-	-	-	-	-
Model B									
NUDS	1.047	1.010, 1.086	0.013*	-	-	-	-	-	-
Global Scale DV	0.935	0.832, 1.052	0.264	-	-	-	-	-	-

NUDS, Normalized Uptake Defect Score; DVDS, DV Defect Score; RI, Retention index; DV, Distribution volume; CI, Confidence Interval.

Table 5:

Comparison of PET Parameter AUC for Predicting SCA up to the median follow-up (4.2 yrs)

Comparison			ΔAUC	95% CI		*p*-Value
Regional NUDS	vs	Regional DVDS	0.00669	−0.0398	0.0532	0.7779
	vs	Global Scale Distribution Volume	0.1256	0.00234	0.2488	0.0458*
	vs	Global Scale Retention Index	0.1310	0.00934	0.2527	0.0348*
Regional NUDS	vs	Global Scale Distribution Volume	0.1189	−0.0111	0.2488	0.0729
	vs	Global Scale Retention Index	0.1243	−0.00372	0.2524	0.0570
Global Scale Retention Index		Global Scale Distribution Volume	−0.00545	−0.1139	0.1030	0.9216
Combined Model						
Regional NUDS	vs	+ Global Scale Retention	−0.00187	−0.0359	0.0322	0.9143
	vs	+ Global Scale Distribution Volume	−0.00156	0.0240	0.0209	0.8920

NUDS, Normalized Uptake Defect Score; DVDS, DV Defect Score

Table 6.

PAREPET Multivariate Model for Time to SCA

Parameter	Hazard Ratio	95% CI	*p*-Value
Per 1 Unit Increase			
Normalized Uptake Defect Score (%LV)	1.045	1.009,1.082	0.0135*
Creatinine (mg/dL)	1.386	1.064, 1.804	0.0153*
Indexed LVEDV (mL/m^2)	1.025	1.010, 1.040	0.0012*
No ACE/ARB	5.770	2.131, 15.623	0.0006*

LVEDV, LV End Diastolic Volume Index; ACE, Angiotensin-converting enzyme; ARB, Angiotensin II Receptor Blocker; CI, Confidence interval.

Table 7.

Net Reclassification Improvement and Integrated Discrimination Improvement for Global PET Parameters to the PAREPET Multivariate Model.

PET Parameter	NRI	*p*-Value	Individuals with event		Individuals without event		IDI	*p*-Value	R^2 Difference
			Up	Down	Up	Down			
Global Scale RI	0.0092	0.8515	0	1	3	9	0.021	0.089	3.17
Global Scale DV	−0.024	0.6204	0	1	4	6	0.0079	0.2961	1.03

*Risk Thresholds for NRI set at 0.9%, 3.9% 11.7% for low, intermediate and high risk, respectively. These are the event rates that correspond to patients with 0 ,1 or >2 high risk parameters (in Table 6).